Tr. J. of Engineering and Environmental Science
23 (1999) , 381 – 388.

Mathematical Modeling of Fractionation During the Mold Filling of Semi-Solid Metal Slurries

Mahmut D.MAT, Kemal ALTINIŞIK, Feridun KARAKOÇ, Yüksel KAPLAN
Mechanical Engineering Department,
Niğde University, 51100, Niğde-TURKEY

Received 08.10.1998

Abstract

Mold filling and fractionation of semi-solid slurries are numerically investigated. A tin lead alloy (Sn-15%Pb) is employed to fill the mold under a range of processing conditions including inflow velocity, mold geometry, nozzle diameter and fraction of the solid. Fractionation is identified from the trajectories of the particles that introduced at the mold inlet. The results showed that phase segregation or fractionation is promoted by the flow and the processing conditions. The fractionation is reduced with a cylindrical mold, high inflow velocity and low fraction of solid.

Key Words: Semi-solid slurries, fractionation, mold filling, mathematical modeling

Yarı-Katı Metal Eriyiklerinin Dökümü Esnasında Ortaya Çıkan Yığılma Olayının Matematiksel Analizi

Özet

Yarı-katı metal eriyiklerinin dökümü ve bu sırada meydana gelen yığılma olayı nümerik olarak incelendi. Kalay-kurşun (Sn-15%Pb) yarı-katı malzemesinin dökümünün simülasyonu, değişik akış hızları, kalıp geometrisi, nozul çapı ve katı faz oran parametreleri dikkate alınarak yapıldı. Yığılma olayı, kalıp içine erimiş malzemeyle giren katı parçacıkların yörüngelerinin takip edilmesiyle tayin edildi. Elde edilen sonuçlar, yığılma olayında akış ve döküm şartlarının son derece önemli rol oynadığını göstermiştir. Özellikle silindirik kalıp kullanılması halinde, yüksek akış hızlarında ve düşük katı faz oranlarında yığılma olayının azaldığı görülmüştür.

Anahtar Sözcükler: Yarı-katı metal eriyikleri, yığılma, döküm, matematiksel modelleme

Introduction

Semi-solid processing involves partially solidifying a melt or partially melting a solid to produce solid particles in a liquid matrix. The solid fraction may vary 20 to 90 percent depending on the application (Brown,1990). Processing of materials in the semi-solid state has received much research interest in recent years due to its potential to manufacture near net shape components. It also has several advantages over the conventional methods. For example, laminar flow during the mold filling operations results in less entrapped gas, leading to less porosity in the final products. The life span of metal dies

is also extended since lower temperatures required relative to casting and reaction between slurry and materials are diminished.

Semi-solid metal slurries exhibit thixotropic behavior, meaning that the viscosity is shear and history-dependent. Flemings and co-workers (1976) studied the rheological characterization of semi-solid slurries, showing that such thixotropic behavior may be represented by a power law constitutive relationship. Nguyen et al. (1992) and Kumar et al. (1993) also concentrated on developing constitutive equations for semi-solid slurries by performing similar experiments. Brown (1990) introduced an internal variable concept which accounts for the evolution of the microstructure of the slurry during the casting process.

Experimental studies have shown that phase segregation occurs during the mold filling of semi-metal slurries (Secordel, 1992; Kolsgaard and Brusethaug, 1993). This phenomenon contributes to the production of unacceptable differential solidification and non-uniform mechanical properties in the solidified product. In the extreme situation choking of mold occurs due to the premature solidification. Although several studies have concentrated on the developing constitutive relationship, relatively few studies have considered the phase segregation. Secordel (1992) found a direct correlation between punch velocity and liquid rejection during the extrusion. However, this study considered only steady state behavior, and the other effects were not investigated.

In this paper, mold filling of semi-solid metal slurries and phase segregation is numerically investigated. A semi-solid slurry is assumed to be a non-Newtonian fluid below a critical solid fraction (f_{crit}), and a viscoplastic medium saturated with liquid phase above the critical solid fraction. A group of particles are introduced at the mold inlet and segregation is studied through the trajectories of these particles. The particles are allowed to change momentum with the continuous phase. The sharp property change at the free surface between the slurry and air is resolved by the Van Leer method (Van Leer, 1977). A range of operations parameters are considered, including inlet velocity, initial solid fraction and mold geometry.

1. Problem Considered

The schematic sketch of the test problem, which consists of two mold-filling systems, is shown in Fig.1. Cylindrical and tapered mold geometries are considered. The cylindrical mold has a uniform internal section, while the other one has a 1° tapering angle. The semi-solid enters from the bottom of the mold and progressively rises in the mold forming a free surface.

The height and radius of the mold are chosen as 0.12 m and 0.025 m respectively. Sn-15%wtPb, which has a density of 7540 kg/m^3, is employed as the semi-solid slurry.

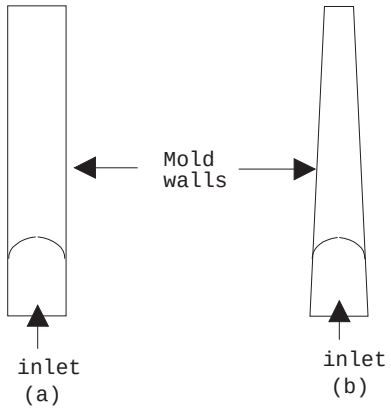

Figure 1. Schematic sketch of test problems considered. (a) cylindrical mold, (b) tapered mold

2. Formulation

A mathematical representation of the mold filling process requires solution of the equations governing the conservation of mass, momentum along with constitutive equation representing the slurry behavior and particle dynamics. A group of particles is introduced at the inlet of mold and the particles are allowed to change momentum with the continuous phase.

The governing equations for a mold filling of a semi-solid system can be expressed in cylindrical coordinates as:

Continuity Equation

$$\frac{\partial w}{\partial t} + \frac{1}{r}\frac{\partial rw}{\partial r} = 0 \tag{1}$$

Axial Momentum

$$\rho\frac{\partial}{\partial t}(w) + \rho\nabla(\mathbf{u}w) = -\frac{\partial p}{\partial z} - (\nabla\tau)_z \tag{2}$$

Radial Momentum

$$\rho\frac{\partial}{\partial t}(v) + \rho\nabla(\mathbf{u}v) = -\frac{\partial p}{\partial r} - (\nabla\tau)_r \tag{3}$$

where **u** is the velocity vector, and v and w are the radial and axial velocities respectively. p is the static τ is the shear stress tensor.

The slurry has an initial solid fraction and behaves as a non-Newtonian flow. A power law relation is employed until a critical solid fraction (f_{crit}) which represent the build up of a solid skeleton occurs. After the critical solid fraction slurry is assumed to be a viscoplastic medium saturated with the liquid phase. The critical solid fraction f_{crit} is chosen as 0.625, which represents the equivalent packing density of spherical particles (Frankel and Acrivos, 1967).

The constitutive relation below the critical solid fraction can be expressed as

$$\mu = m \left| \frac{1}{2} (\Delta : \Delta)^{1/2} \right|^{n-1} \tag{4}$$

where Δ is the rate of deformation tensor. Δ:Δ is the dyadic product of Δ and expressed as:

$$\frac{1}{2}\Delta{:}\Delta = 2\left[\left(\frac{\partial w}{\partial z}\right)^2 + \left(\frac{\partial v}{\partial r}\right)^2 + \left(\frac{\partial w}{\partial r} + \frac{\partial v}{\partial z}\right)^2 \right] \tag{5}$$

m and n are empirical coefficients and defined as:

$$m = exp(9.283 f_s + 1.435) \tag{6}$$

$$n = \left\{ \begin{array}{ll} 0.1055 + 0.41 f_s & f_s < 0.30 \\ -0.308 + 1.28 f_s & f_s \geq 0.30 \end{array} \right\} \tag{7}$$

The relations (6, 7) for the empirical coefficient were developed by Joly (1974).

Above the critical solid fraction the slurry is assumed to be a viscoplastic medium saturated with liquid phase. The constitutive relation above f_{crit} is adapted from a recent work of Ilegbusi and Mat (1998) as follows:

$$\mu = 2v^{(1-n)n} \alpha^{-1} \beta^{-1/n} A(f_s)^{-(1+n)/2n} exp(\frac{-Q}{RT}), + e f_s^n exp(-ct) \gamma^{(n-1)/n} \tag{8}$$

where α, β c and e are empirical constants that depend on the material, γ is the shear rate, Q is the activation energy, R is the universal gas constant and n is the power law constant. $A(f_s)$ is a function that represents the microstructure. Martin et al. (1995) proposed the following relation for a globular microstructure:

$$A(f_s) = \frac{3.0}{f_s^{15}} \tag{9}$$

Since the problem is solved under isothermal conditions, f_s in Eqs. 6-8 is assumed to be constant, and the corresponding T in Eq. 8 is calculated assuming f_s varies linearly between liquidus (T_{liq}) and eutectic (T_e) temperatures of Sn-15%wt Pb alloy. The values of the data used in the calculations are given in Table 1.

2.1. Particle Physics

The evolution of the particle position Z_p is determined from the solution of the following equation:

$$\frac{dZ_p}{dt} = w_p \tag{10}$$

in which w_p is the particle velocity vector, obtained from the following particle momentum equation:

Table 1. Values of Data Used in Calculations

Symbol	Value	Units	Reference
α	0.03	MPa^{-1}	Martin et al. (1995)
β	4.5×10^{-2}		Martin et al. (1995)
c	0.1	s	Ilegbusi and Mat (1998)
e	140.5	1/s	Ilegbusi and Mat (1998)
n	5.7		Martin et al. (1995)
Q	257	kj/kg	Martin et al. (1995)
R	8.13	kj/kgK	Martin et al. (1995)
ρ	7540	kg/m^3	Ilegbusi and Mat (1998)
T_e	456	K	Kumar et al. (1993)
T_{liq}	483	K	Kumar et al. (1993)

$$m_p \frac{dw_p}{dt} = D_p(w - w_p) + m_p b_g - V_p \nabla p \quad (11)$$

where m_p is the mass of a particle, D_p is the drag function, V_p is the volume of particle, p is the pressure, w is the continuous phase velocity and b is the buoyancy factor.
Drag function D_p can be expressed as (Fueyo et al.,1992):

$$D_p = \frac{1}{2}\rho_p A_p C_D |w - w_p|^2 \quad (12)$$

where A_p is the particle projected area and C_D is the drag coefficient. C_D is calculated from a correlation by developed Clift et al. (1978):

$$C_D = \frac{24}{Re}(1+0.15Re^{0.687}) + \frac{0.42}{1.425.10^4 Re^{-1.16}} \quad (13)$$

where Re is a particle Reynolds number defined as;

$$Re = \frac{|w_p - w_c| d_p}{\nu} \quad (14)$$

where ν is the kinematic viscosity of the continuous phase and d_p is the particle diameter.
The buoyancy factor is given as:

$$b = (1 - \frac{\rho_c}{\rho_p}) \quad (15)$$

2.2. Initial and Boundary Conditions

The mold is initially assumed to be filled with a quiescent gas (air). The semi-solid slurry is allowed to fill the mold at t>0. Only half of the mold is considered due to symmetry at the mold axis. The mold wall is assumed to be impermeable and a no-slip condition to be valid on the wall. The initial and boundary conditions can be expressed mathematically as

$$t = o : v = w = 0 \quad (16)$$

$$t > 0 \; at \; r = 0 : \frac{\partial w}{\partial r} = \frac{\partial v}{\partial r} = 0 \quad (17)$$

$$at \; r = r_0 : v = w = 0 \quad (18)$$

$$at \; z = 0 : w = V_{in} \quad (19)$$

3. Numerical Method

The governing equations are solved numerically with a fully implicit, finite domain scheme embodied in the PHOENICS (Rosten and Spalding,1986) code. Since the mold filling operation involves a free surface or the interaction of two distinct media (slurry and gas) separated by sharply deformed interfaces, the discretization of the governing equation with a conventional upwind scheme usually results in a false numerical diffusion, which leads to unphysical results. Therefore, a van Leer scheme (Van Leer,1977) is employed to resolve such property interface.

Due to the coupling between the transport equations governing the continuous phase and particles, a three-step solution procedure is employed. In the first step, the continuous-phase equations are solved assuming there is no particles. The next step follows the integration of particle equations using the current value of continuous phase velocity and calculation of the inter-phase sources. The continuous phase equations are solved again including the particles in the last step. This procedure is repeated until a converged solution is obtained.

A 50×30 grid system is employed in all computations. This grid system and a uniform time step of 0.001 s is found to be sufficiently refined for a numerically accurate result. A typical calculation requires approximately 2 hours of CPU time on a Pentium personal computer.

4. Results

Several effects can be investigated in this problem; however only the effects of mold geometry, inlet velocity and solid fractions are considered. Seventy-five percent of the inlet area is employed as the nozzle by which the semi-solid enters the mold in all cases. The cases considered in this study are summarized in Table 2.

Table 2. Cases Considered

case#	V_{in}(m/s)	f_s	mold geometry
1	0.2	0.5	cylindrical
2	0.2	0.5	tapered
3	0.2	0.5	cylindrical
4	0.3	0.5	cylindrical
5	0.4	0.5	cylindrical
6	0.2	0.6	cylindrical
7	0.2	0.7	cylindrical

Figure 2 shows the evolution of the slurry interface and velocity profiles for the cylindrical mold at time spans of t=0.1, 0.5 and 0.9 sec. for f_s=0.5 and V_{in}=0.2 m/s. Only half of the mold is illustrated due to the symmetry. It is seen that slurry interface exhibits a jetting characteristics which increases as filling progresses. The velocity profile is higher at the axis while lower at the mold walls.

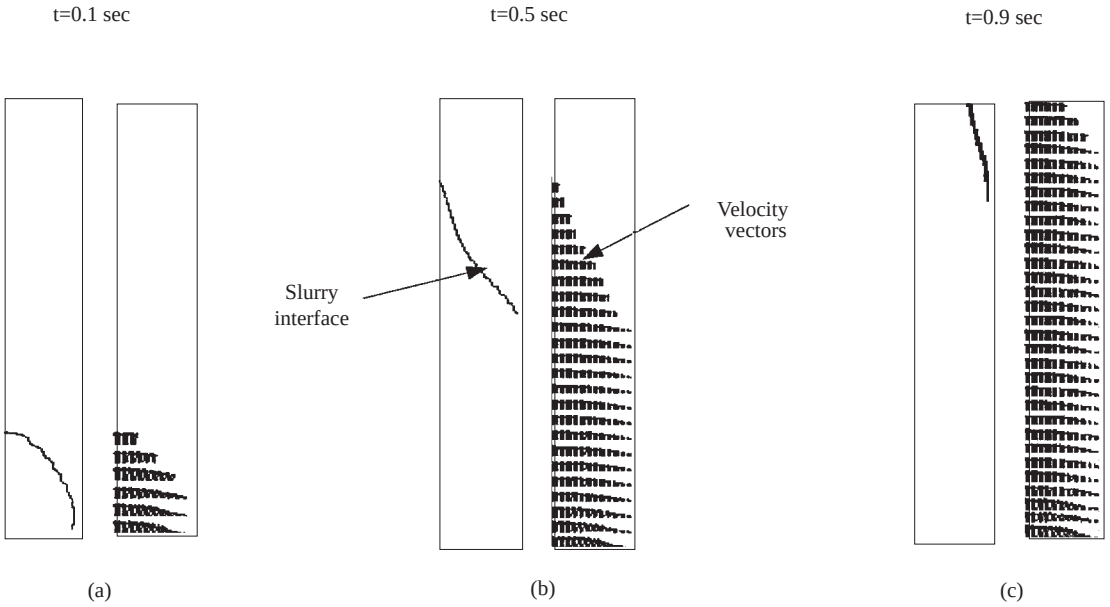

Figure 2. Advance of slurry interface and corresponding velocity profiles for cylindrical mold (f_s=0.5, V_{in}=0.2 m/s)

Trajectories of the representative particles are shown in Fig. 3. Particle trajectories for the tapered mold are also included in Fig. 3b along with the cylindrical mold. The evolution of slurry interface and velocity profiles for the tapered mold are not illustrated due to space limitations.

It is seen that a portion of particles continuously attaches to the wall as the filling progresses. Significant fractionation occurs before the slurry reaches the top of the mold. The extent of the fractionation is generally lower in the cylindrical mold.

Figure 4 shows the effect of mold geometry on the axial variation of the fractionation. H represents the height of the mold in this and subsequent figures. The fractionation is quantified from the following relation:

$$\eta = 1 - \frac{\sum N}{N_0} \tag{20}$$

where N_o is the total number of particles introduced at the inlet and $\sum$N is the predicted sum of the all particles that reached the top of the mold.

It is seen that fractionation is higher in the tapered mold than in the cylindrical mold. This is the result of tapered mold walls that prevent motion of the particles, and recirculation zones that develop near the walls. This result has practical importance since a tapering angle of even 1° causes significant fractionation in the mold.

Figure 3. Particle trajectories for cylindirical and tapered molds: (a) cylindrical mold, (b) tapered mold (V_{in}=0.2 m/s, f_s=0.5)

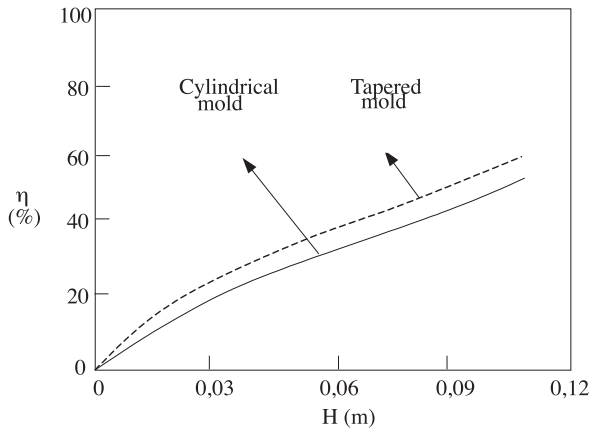

Figure 4. Effect of mold geometry on the axial variation of the fractionation (V_{in}=0.2 m/s, f_s=0.5)

Figure 5 shows the axial fractionation in a cylindrical mold at three values of inflow velocities: 0.2 m/s, 0.3 m/s and 0.4 m/s. It is seen that the fractionation decreases at higher inflow velocities. This trend may be the result of the lower residence time of slurry in the mold as well as the larger inertia and drag forces on all slurry phases as the velocities increase.

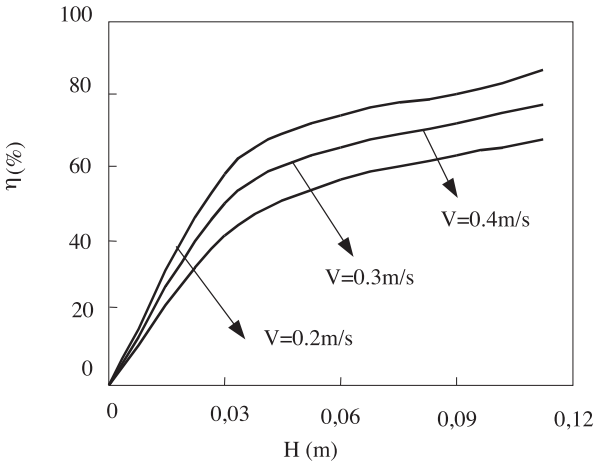

Figure 5. Effect of inflow velocity on axial fractionation (f_s=0.5, cylindrical mold)

The effect of solid fraction on axial fractionation is shown in Fig. 6. It is seen that fractionation increases considerably with the solid fraction. This trend is the result of high shear stresses developed at higher solid fractions. Figure 7 shows that the time required to fill the mold also increases with the higher solid fractions. While it takes approximately 1 sec to fill a cylindrical mold with f_s=0.5, 2.5 sec are required to fill the same mold with slurry with the 0.7 solid fraction.

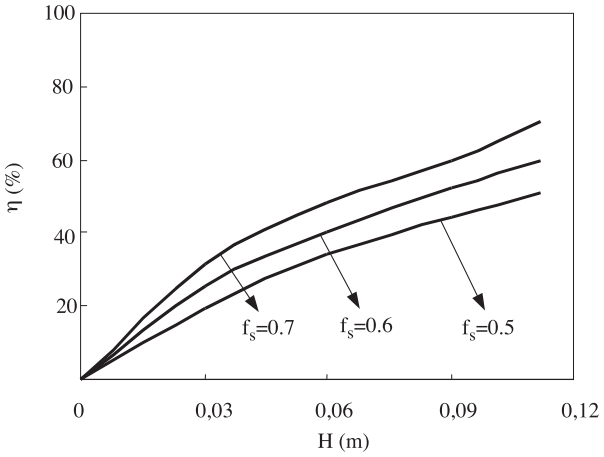

Figure 6. Effect of solid fraction on axial fractionation (V_{in}=0.2 m/s, cylindrical mold)

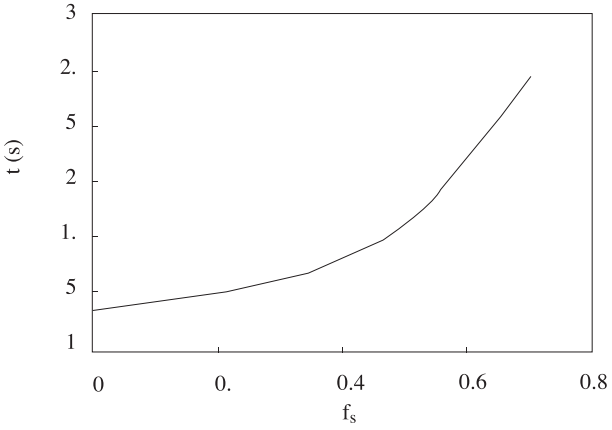

Figure 7. Effect of solid phase fraction on filling time (V_{in}=0.2 m/s, cylindrical mold)

5. Conclusions and Discussion

Fractionation during the mold-filling operations of a semi solid slurry is numerically investigated. The effects of mold geometry and a range of processing conditions including mold geometry, inflow velocity, solid fraction are considered. The fractionation is

determined from the trajectories of particles introduced at the mold interface.

The major finding of this study is that the fractionation is strongly dependent on the mold geometry and processing conditions. The numerical results show that use of a cylindrical mold results in less fractionation in the final product than that of the tapered mold which prevents motion of the particles. It is found that higher punch velocities reduce fractionation due to the lower residence time of particles in the mold. Higher solid fractions are found to increase the fractionation and mold filling time.

The practical implication of the results is that a rapid mold filling with a smooth geometry is required to manufacture advanced engineering components with lower phase segregation. The jetting characteristics of the slurry interface indicates a complex structure that develops in non-Newtonian flow. This study considers relatively simple geometry however, it provides useful information for understanding the fundamentals of fractionation. It can easily be extended to complex geometries.

6. Nomenclature

A	particle projected area, m^2
c	viscosity constant in Eq. 8, s
C_D	drag coefficient
d	particle diameter, m
D	drag function, N
e	viscosity constant in Eq.8, 1/s
f_s	solid fraction
f_{crit}	critical solid fraction
H	mold height, m.
m	mass, kg
n	viscosity coefficient in Eqs.4 and 7; power law constant in Eq. 8
N	number of particles
p	static pressure, N/m^2
Re	Reynolds number
r	radial coordinate, m.
r_o	radius of mold, m
Q	activation energy, j/kg
R	universal gas constant, j/kgK
t	time, s
v	radial velocity, m/s
V_{in}	inlet velocity, m/s
w	axial velocity, m/s
z	axial coordinate, m
α	Viscosity constant in Eq. 8, 1/Pa
β	Viscosity constant in Eq. 8,
γ	shear rate, 1/s
Δ	deformation tensor, 1/s
η	fractionation
μ	viscosity, Ns/m^2
ρ	density, kg/m^3
τ	shear stress, N/m^2

6.1. subscript

c	continuous phase
p	particle

References

Brown, S., "An Internal Variable Constitutive Model for Semi-Solid Slurries", Proc. 5^{th} Int. Conference Modeling of Casting, Welding and Advanced Solidification Processes (Davos, Switzerland), TMS, 31-38, 1990.

Clift, R., Grace, J. R., and Weber, M. E., Bubbles, Drops, and Particles, Academic Press New York, 1978.

Flemings, M. C., Riek, R. G. and Young, K. P., " Rheocasting Processes", AFS in Cast Metals Jour., 11-19, 1976.

Frankel, N. A. and Acrivos, A., "On the Viscosity of a Concentrated Suspension of Solid Spheres", Chemical Engineering Science 22, 847-853, 1967.

Fueyo, N., Hamill, I., and Zhang, Q., The GENTRA User Guide, CHAM Limited (UK) Technical Report, TR/211, 1992.

Ilegbusi, O. J., and Mat, M. D., "Internal-Variable Constitutive Model for Semi-Solid Slurries at High Solid Fractions", J. Materials Engineering and Performance, V 7, 199-204, 1998.

Joly, P.A., Ph.D. Thesis, Department of Materials Science and Engineering, M.I.T., 1974.

Kolsgaard, A., and Brusethaug, S., " Settling of SiC Particles in a AlSi7Mg Melt", Materials Science and Engineering, A173, 213-219, 1993.

Kumar, P., Martin, C. L., and Brown, S., " Shear Rate Thickening Flow Behavior of Semi-Solid Slurries", Metallurgical Trans. 24A, 1107-1116, 1993.

Laxmanan, V., and Flemings, M. C., " Deformation of Semi-solid Sn-15% Pb Alloy," Metal. Trans. A,1IA, 1927-1937, 1980.

Martin C. L., Brown, S. B., Favier, D., and Suery, M., "Shear deformation of high solid fraction (> 0.60)

semi-solid Sn-Pb under various structures", Mater. Sci. & Eng., A202:11-122, 1995.

Nguyen, T. G., Suery, M., and Favier, D., " Mechanical Behavior of Semi-Solid Alloys Under Drained Compression with Lateral Pressure", in Proc. 2nd Int. Conf. on Processing of Semi-Solid Alloys and Composites, Boston, MA, 296-304, June 10-12, 1992.

Rosten, H., and Spalding, D.B., PHOENICS Beginner's Guide and User's Manual, CHAM Limited (UK) Technical Report, TR/100, 1986.

Secordel, P. and Valette, E., " Experimental Extrusion Test to Study the Rheological Behavior of Semi-Solid Steels", Proceedings of the Second International Conference on the Processing of Semi-Solid Alloys and Composites, M.I.T., Cambridge, Massachusetts, USA, 306-315, June 10-12, 1992.

Van Leer, B., "Towards the ultimate conservative difference scheme. IV. A new approach to numerical convection", J. Computational Phys., 23, 276-299, 1977.